Preprints of the 21st IFAC World Congress (Virtual)
Berlin, Germany, July 12-17, 2020

Robust Data-driven Estimation of Wave Excitation Force for Wave Energy Converters

Shuo Shi [*,**] **Ron J. Patton** [*] **Yanhua Liu** [*]

[*] *Department of Engineering, University of Hull, Cottingham Road, Hull, HU6 7RX, UK (e-mail: S.Shi-2016@hull.ac.uk, r.j.patton@hull.ac.uk, Y.Liu@hull.ac.uk).*
[**] *State Grid Shandong Electric Power Research Institute, China.*

Abstract: This paper proposes a data-driven technique to estimate the wave excitation force (WEF) which is an essential signal for wave forecasting and implementing power efficiency maximization control of Wave Energy Converters (WECs). A Bayesian probabilistic model of a WEC hydrodynamic system is described to generate robust WEF estimates. Specifically, the WEF uncertainty can be estimated based on observations through Gaussian Process (GP) modeling. It is shown that this modern way of incorporating the first principle modelling into a probabilistic framework has stronger robustness properties than the alternative of calculating estimates of a parametric function representation. Unlike the sample-based non-linear Kalman Filter, the means and covariances of the joint probabilities can be directly computed based on analytic moment matching that allow for reliable state-dependent uncertainty propagation. The results presented demonstrate the accuracy and robustness of the proposed data-driven wave excitation force estimator.

Keywords: Wave excitation force estimation, Gaussian process, Kalman filter, Sparse identification, Wave energy

1. INTRODUCTION

Wave energy has a great potential for development and forms an indispensable part of marine renewable energy (Association et al., 2010), representing higher energy density compared to offshore wind energy. However, compared to wind turbine technology Wave energy converters (WEC) are still at an early stage of development due to the low (achieved) energy conversion efficiency and high maintenance requirements. The development of the wave energy requires optimizing the conversion of the resources to reduce the Levelized Cost of Energy (LCoE). Optimal control (Ringwood et al., 2014) can maximize the conversion efficiency by driving the WEC into approximate resonance with the wave excitation force of the incoming waves.

The majority of the proposed energy maximizing control methods require the instantaneous and predicted information of the wave excitation force F_{ex} as the determination inputs (Faedo et al., 2017). Whereas the performance of some other well-known control strategies including complex-conjugate control (Salter et al., 2002), latching control (Budal and Falnes, 1977) are strongly affected by the knowledge of the future wave elevation η. However, in a real multi-directional sea scenario, obtaining accurate η measurements at the position WEC has been installed is a non-trivial task (Shi et al., 2019). Attractively, the WEF estimator provides an interesting alternative of obtaining reliable η measurements at the location of the WEC. The η can be computed via Fourier transform of the Frequency Response Function (FRF) of the F_{ex}. Hence, the WEF estimator can be served as a redundant system to the wave gauges, with an ability to provide more accurate wave forecasting performance (Ling, 2019). Only few casual control algorithms, such as simple and effective real-time control (Fusco and Ringwood, 2013), learning-based prediction-less resonating controller (Shi et al., 2019) do not rely on the knowledge of η or F_{ex}.

In the real operational scenario, WEF is un-measurable, therefore, extensive research is currently being conducted on the WEF estimation problem and on which several methods have been proposed. Recently, the paper (Peña-Sanchez et al., 2019) performs a comparison of all current available WEF estimators found in the literature. According to the required measurements, there are three distinct classes of estimators: using η measurements, using device motion measurements, or using both device motion and pressure measurements. The performance of using η measurements only is heavily affected by both the accuracy of the η prediction which is not considered reliable for real (irregular) sea operation (Shi et al., 2018), and also the definition of the $IRF_{F_{ex}}$. Furthermore, to obtain reliable η measurements requires several wave gauges (as stated above), due to the principle that η is physically un-measurable at the device location. Hence, it is found that the second group of WEF estimators based on sole use of device motion measurements is the most practically feasible technique, specifically the Kalman Filter with Harmonic Oscillator method (Ling, 2019) and Unified Linear Input and State Estimator (Coe and Bacelli, 2017) and

the robust unknown input observer (UIO) (Abdelrahman and Patton, 2019), represent better overall performance in terms of accuracy and delay time over other estimation strategies. There is no evidence that including pressure measurements could provide additional advantage. Indeed, the UIO estimator described by (Shi et al., 2019) and in detail by (Abdelrahman and Patton, 2019) is the only approach able to take model uncertainty into account, which is important to the robust control of WEC in the real practice. However, most WEF estimators are based on linear modeling technique, which belies the true non-linear hydrodynamics of WECs in the ocean.

This paper propose a novel robust WEF estimator that can handle both model uncertainty and non-linearity of WEC hydrodynamic. In contrast to the use of other Gaussian filters such as Kalman Filter, in which the process and measurement noise should be specified, the proposed estimator can learn these properties together with other system uncertainty directly from data through probabilistic modeling technique. In particular, the sparse identification of non-linear dynamics (SINDy) modeling procedure is adopted to approximate the WEC first principles physics model, and an non-parametric Gaussian Process (GP) model quantifies the unknown dynamics of the WEC system. Based on this statistical model, the calculation of state-dependent uncertainty becomes feasible by using reliable uncertainty propagation technique that approximates the intractable *posterior* of the GP probabilistic model with uncertain inputs by another Gaussian. Hence, the means and co-variances of joint probabilities can be analytically computed. This data-driven method estimates the WEF in a more robust and practical way by incorporating the first principle model and unknown uncertainty within a probabilistic framework.

2. PROBLEM STATEMENT

The floater-wave dynamics are often calculated by solving the Cummins' equation (Cummins, 1962):

$$m^*a(t) + F_r(t) + F_v(t) + F_h(t) + F_{pto}(t) = F_{ex}(t) \quad (1)$$

where $m^* = m + A_\infty$, m is the floater mass, A_∞ is the added mass at infinite wave frequency, $a(t)$ is the acceleration vector of the floater, F_r is the radiation force, $F_{ex}(t)$ is the wave-excitation force, $F_h(t)$ is the hydrostatic restoring force, $F_{pto}(t)$ is the force exerted by (Power Take Off) PTO system, $F_v(t)$ is the viscous force. Equation (1) can be approximated by the following deterministic, discrete-time dynamical system:

$$\begin{aligned} x_{k+1} &= f(x_k, u_k) + w_k \\ &= \underbrace{h(x_k, u_k)}_{\text{prior model}} + \underbrace{g(x_k, u_k) + w_k}_{\text{unknown uncertainty}} \end{aligned} \quad (2)$$

where $x_k = [p_k \ v_k \ a_k \ F_{exk}]^T$, p_k and v_k denote the floater position and velocity, respectively. $u_k = F_{pto_k}$ is the control input to the system at time k.

Usually, the *prior* model h in the WEF estimator are inaccurately identified based on linear model. In this work, the *prior* model is represented by an non-linear parametric model which has been identified through the SINDy modeling procedure. The unknown uncertainty relates to both the un-modeled dynamics g and process noise $w_k \sim \mathcal{N}(0, \sigma^2)$, the noise covariance matrix is Q. In order to reduce these unknown uncertainties and learn the unmodelled dynamics g, a probabilistic model is adopted, whose mean and covariance are given by Gaussian approximations $\mathcal{N}(x_k|\mu_{k|\tau}, \Sigma_{k|\tau})$, where a subscript τ abbreviates $1, ..., k$. This work computes the input-dependent $\mu_{k|\tau}$ and corresponding uncertainty estimates $\Sigma_{k|\tau}$ based on the GP model. It should be noted that GP model can learn the un-modeled dynamics, hence reducing the unknown uncertainty which is quantified by GP as well. Noticeably, unlike other estimators such extended Kalman Filter, the process noise matrix Q becomes state dependent covariance matrix to describe both process uncertainty (un-modeled dynamics) and process noise in the GP model, no longer require tuning through error-trial method. Although, the similar modeling structure in Equation (2) could be used to represent the system observations, a simple discrete-time state-space model is adopted here due to the simplicity of the system measurement function:

$$z_k = Cx_k + \epsilon_k \quad (3)$$

where $z_k = [p_k \ a_k]^T$, ϵ_k is the measurement noise, whose covariance matrix is R, $C \in \mathbb{R}^{q \times n}$ is given by

$$C = \begin{bmatrix} 1 & 0 & 0 & 0 \\ 0 & 0 & 1 & 0 \end{bmatrix}$$

The matrix C selects the position and acceleration of the device as outputs. The *prior* distribution $p(x_0)$ of the initial state x_0 is $\mathcal{N}(\mu_0, \Sigma_0)$, and the purpose of the WEF estimator is to find approximations of the *posterior* distributions $p(x_k|z_{1:k})$.

3. SPARSE IDENTIFICATION OF NON-LINEAR DYNAMICS

SINDy combines a library of candidate non-linear terms and sparsity-promoting regression to identify non-linear dynamical systems from the time-series data(Brunton et al., 2016). Although, there are many data-driven modeling approaches to discover the system dynamics, these learning-based algorithms often suffer from over-fitting, inability of interoperability and the reliance on massive data sets. By contrast, the SINDy framework allows the incorporation of known physics to construct a combinatorially large library of possible non-linear functions. Based on a sparsity-promoting optimization, a parsimonious model is sparsely selected from the library based on limited data, resulting in interpretable models that avoid over-fitting problem. The SINDy model could represent the complex system with as few non-linear terms as possible. In the SINDy framework the dynamical systems of the form

$$x_{k+1} = f(x_k, u_k) = \sum_{l=1}^{\zeta} \xi_l h_l(x_k, u_k) \quad (4)$$

where the sum of functions $\sum_{l=1}^{\zeta} \xi_l h_l$ describes how the state evolves in a time step. The small ζ indicates that the system dynamics can be identified by a parsimonious set of functions. In order to sparsely select these unknown functions, a comprehensive library of candidate functions $\Theta(x, u) = [h_1(x, u)h_2(x, u), \cdots, h_p(x, u)]$ need to be constructed, so the functions in Equation (4) are the subset of $\Theta(x, u)$. The choice of library functions is crucial to the performance of the SINDy algorithm. One conservative strategy is to begin with polynomials

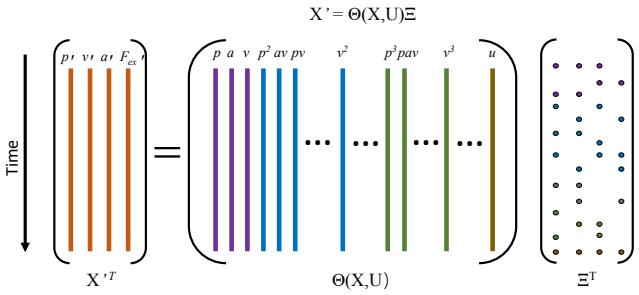

Fig. 1. Schematic of the SINDy algorithm

and then gradually increase the complexity of functions by adding other terms, such as trigonometric functions. Importantly, it is also possible to incorporate partially known physics into the library candidate function. For the wave energy scenario, some terms in Equation (1) are known, $F_h(t) = K_h p(t)$, K_h is the hydrostatic coefficient, $F_v(t) = K_v v(t) + K_d v(t)\,|(v(t))|$, K_d, K_v are the viscous coefficients, the non-linear F_v is often ignored but very important. It is worth noting that nearly all the non-linear forces exerted on the WEC can be approximated by product combination of the states in x and the corresponding coefficients, which construct the main library candidate functions for the SINDy model of the WEC. Hence, SINDy modeling technique has the potential to capture more non-linear dynamics than a linear model due to extra non-linearity is considered in the library. The radiation force $F_r(t)$ can be approximated using a parametric state space model(Taghipour et al., 2008), which can be added into the library candidate function in the future work to improve the SINDy performance. The training data sets are arranged according to the state matrix $X \in \mathbb{R}^{m\times n}$ and control vector $U \in \mathbb{R}^m$. Then the function library $\Theta(X,U) \in \mathbb{R}^{m\times p}$ is evaluated for all observations. The corresponding next time step state matrix $X' \in \mathbb{R}^{m\times n}$, is collected with the columns of X by moving advanced one observation:$X' = [x_2 x_3 ... x_{m+1}]$. Then the Equation (4) can be written as:

$$X' = \Theta(X,U)\Xi \tag{5}$$

where the $\Xi \in \mathbb{R}^{p\times n}$ contains the unknown coefficients that need to be solved. It is should be noted that the ith column of Ξ determines the sparsity and accuracy of the ith state variable. For each coefficient vector in Ξ, it is expected that as few elements are non-zero as possible, such that only a small number of candidate functions could give good model performance. Therefore, sparsity-promoting regression is employed to identify Ξ :

$$\min_{\Xi} \frac{1}{2}||X' - \Theta(X,U)\Xi||_2^2 + \lambda||\Xi||_0 \tag{6}$$

Here, the sparse-coefficient can be solved by using the Lagrangian minimization problem, $||.||_0$ is a regularizing function to promote sparsity in Ξ, λ is a free parameter that governs the magnitude of the sparsity penalty. In this work, the sequentially thresholded least-squares approach is adopted to compute this minimization problem, where any elements in the coefficient vector less than a threshold λ are set to zero in each iteration. The schematic of the SINDy algorithm can be seen in Fig.1, where active terms are identified through spare-promoting regression in a library of candidate functions.

4. GAUSSIAN PROCESS WITH UNCERTAIN INPUT

GP is a popular Bayesian non-parametric method, which has been successfully used in both machine learning and control science. The appeal of using GP for model identification stems from the fact that it is able to approximate the arbitrary continuous functions with uncertainty quantification that rely on only a small amount of *prior* process knowledge about the modeled system in a very limited data scenario. As its flexibility and inherent ability to measure uncertainty in system estimation, we adopt the GP here to model the unknown dynamics and errors, consequently reducing the system uncertainty and providing direct assessment of the state-dependent uncertainty. Formally, a GP is a random process involving an infinite set of variables, any finite subsets of which are jointly Gaussian distributed(Rasmussen and Williams, 2006). State and control measurements form the input data to the GP and the corresponding training targets are computed from the deviation to the *prior* model:

$$y_k = g(x_k, u_k) + w_k = x_{k+1} - h(x_k, u_k)$$

With $\tilde{x} = [x^T u^T]^T$, the GP model can be fully specified by a mean function $m(\cdot)$ and a covariance function $k(\cdot,\cdot)$, we write $g \sim \mathcal{GP}$ to indicate that the latent function g is GP distributed. Throughout this article, the covariance function is the squared exponential (SE), given by:

$$k(\tilde{x}_i, \tilde{x}_j) = \alpha^2 exp(-\frac{1}{2}(\tilde{x}_i - \tilde{x}_j)^T \Lambda^{-1}(\tilde{x}_i - \tilde{x}_j)) \tag{7}$$

where Λ is a positive diagonal length-scale matrix and α is the output scale. However, it is straightforward to use other differentiable kernels. Generally, the zero-mean function is assumed, with the training input $\widetilde{X} = [\tilde{x}_1, \cdots, \tilde{x}_m]$, the corresponding training targets $Y = [y_1, \cdots, y_m]^T$, the *posterior* predictive distribution of $g_* = g(\tilde{x}_*)$ for an arbitrary test $\tilde{x}_*$ is given by(Rasmussen and Williams, 2006):

$$\mu_g(\tilde{x}_*) = k(\tilde{x}_*, \widetilde{X})[K + \sigma^2 I]^{-1} Y = k_*^T \beta \tag{8}$$

$$\sigma_g^2(\tilde{x}_*) = k(\tilde{x}_*, \tilde{x}_*) - k_*^T [K + \sigma^2 I]^{-1} k_* \tag{9}$$

in which, $k_*^T = k_* = [k(\widetilde{X}_1, \tilde{x}_*), \cdots, k(\widetilde{X}_m, \tilde{x}_*)]$, $\beta := [K + \sigma^2 I]^{-1} Y$, and K is the covariance matrix with $K_{ij} = k(\tilde{x}_i, \tilde{x}_j)$. However, by evaluating the *posterior* distribution of a GP from an uncertainty input $\tilde{x}_* \sim \mathcal{N}(\mu, \Sigma)$, the resulting distribution is generally not Gaussian:

$$p(g(\tilde{x}_*)|\mu, \Sigma) = \int p(g(\tilde{x}_*)|\tilde{x}_*) p(\tilde{x}_*|\mu, \Sigma) d\tilde{x}_* \tag{10}$$

The μ_g and σ_g^2 of the predictive distribution for $p(g(\tilde{x}_*)|\tilde{x}_*)$ can be obtained from Equations (8) and (9), respectively. For the SE kernel, the mean μ_* and σ_*^2 of Equation (10) can be computed in closed form(Deisenroth et al., 2009):

$$\mu_* = \int \mu_g(\tilde{x}_*) \mathcal{N}(\tilde{x}_*|\mu, \Sigma) d\tilde{x}_* = \beta^T \Gamma \tag{11}$$

with $\Gamma = [\gamma_1, \cdots, \gamma_m]^T$, where

$$\gamma_i = \int k(\tilde{x}_i, \tilde{x}_*) p(\tilde{x}_*) d\tilde{x}_* = \alpha^2 |\Sigma\Lambda^{-1} + I|^{-\frac{1}{2}} \times exp(-\frac{1}{2}(\tilde{x}_i - \mu)^T (\Sigma + \Lambda)^{-1}(\tilde{x}_i - \mu))$$

The variance σ_*^2 is

$$\sigma_*^2 = \beta^T L \beta + \alpha^2 - tr([K + \sigma^2 I]^{-1} L) - \mu_*^2 \tag{12}$$

where $tr(\cdot)$ is the trace of matrix and with $\tilde{x}_{ij} := \frac{1}{2}(\tilde{x}_i + \tilde{x}_j)$

$$L_{ij} = \frac{k(\tilde{x}_i, \mu)k(\tilde{x}_j, \mu)}{|2\Sigma\Lambda^{-1} + I|^{\frac{1}{2}}} \times exp((\tilde{x}_{ij} - \mu)^T(\Sigma + \frac{1}{2}\Lambda)^{-1}\Sigma\Lambda^{-1}(\tilde{x}_{ij} - \mu))$$

Therefore, the intractable posterior predictive distribution $p(g(\tilde{x}_*)|\mu, \Sigma)$ of the GP probabilistic model with uncertain inputs has been approximated by another Gaussian $\mathcal{N}(\mu_*, \sigma_*^2)$, with explicit reliance on the mean and covariance of the input distribution.

Now, to extend the previous results to the multivariate prediction scenario, where N GP models have been independently trained with same input $\tilde{X}$, but different training targets $Y_a = [y_1^a, \cdots, y_m^a]^T$, $a = 1, \cdots, N$. For a deterministically input $\tilde{x}_*$ and an uncertain input $\tilde{x}_* \sim \mathcal{N}(\mu, \Sigma)$, the mean μ_* and variance σ_*^2 of a GP model for each state dimension are given by Equations (8)-(9), and Equations (11)-(12), respectively. However, the predictive covariance matrix of $p(g(\tilde{x}_*)|\mu, \Sigma)$ is no longer diagonal, and only the variance on the diagonal can be collected from N individual predictions. The cross-covariances between target dimensions are given by

$$\begin{aligned} cov[g_*^a, g_*^b|\mu, \Sigma] &= E_{g,\tilde{x}_*}[g_*^a, g_*^b|\mu, \Sigma] - \mu_*^a\mu_*^b \\ &= \beta_a^T\widetilde{L}\beta_b - \mu_*^a\mu_*^b \end{aligned} \tag{13}$$

where $a, b \in 1, \cdots, N$, $g_*^a := g^a\tilde{x}_*$, and $\beta_a := [K_a + \sigma_a^2 I]^{-1}Y_a$, with $\Psi := (\Lambda_a^{-1} + \Lambda_b^{-1})^{-1} + \Sigma$,

$$\begin{aligned} \widetilde{L}_{ij} =& \alpha_a^2\alpha_b^2|(\Lambda_a^{-1} + \Lambda_b^{-1})\Sigma + I|^{\frac{1}{2}} \\ & \times exp(-\frac{1}{2}(\tilde{x}_i - \tilde{x}_j)^T(\Lambda_a + \Lambda_b)^{-1}(\tilde{x}_i - \tilde{x}_j)) \\ & \times exp(-\frac{1}{2}(\tilde{x}_{ij} - \mu)^T\Psi^{-1}(\tilde{x}_{ij} - \mu)) \\ \tilde{x}_{ij} :=& \Lambda_b(\Lambda_a + \Lambda_b)^{-1}\tilde{x}_i + \Lambda_a(\Lambda_a + \Lambda_b)^{-1}\tilde{x}_j \end{aligned}$$

With these results, the mean μ_* and the covariance Σ_* of $p(g(\tilde{x}_*)|\mu, \Sigma)$ can be computed analytically. It is worth noting that the calculations of μ_* and Σ_* are based on both previous state and observations in training data set, resulting in more robust and consistent performance.

5. A GENERAL PERSPECTIVE ON BAYESIAN FILTERS

As mentioned in Section 2, given a *prior* distribution $p(\tilde{x}_0) = \mathcal{N}(\mu_0, \Sigma_0)$ of the initial state, the purpose of the filter is to find approximations of the posterior distributions $p(\tilde{x}_k|z_{1:k})$. Noting that the initial state and filtered state both include control signal u, due to the requirement of uncertainty propagation for GP model. Using the Bayesian theorem, the filter distribution at time k is

$$p(\tilde{x}_k|z_{1:k}) = \frac{p(\tilde{x}_k, z_k|z_{1:k-1})}{p(z_k|z_{1:k-1})} \propto p(z_k|\tilde{x}_k)p(\tilde{x}_k|z_{1:k-1}) \tag{14}$$

Bayesian filters approximate the distribution $p(\tilde{x}_k|z_{1:k})$ via a Gaussian distribution $\mathcal{N}(\mu_k^{\tilde{x}}, \Sigma_k^{\tilde{x}})$, which are generally obtained through(Deisenroth and Ohlsson, 2011)

$$\mu_k^{\tilde{x}} = \mu_{k|k-1}^{\tilde{x}} + \Sigma_{k|k-1}^{\tilde{x}z}(\Sigma_{k|k-1}^z)^{-1}(z_k - \mu_{k|k-1}^z) \tag{15}$$

$$\Sigma_k^{\tilde{x}} = \Sigma_{k|k-1}^{\tilde{x}} - \Sigma_{k|k-1}^{\tilde{x}z}(\Sigma_{k|k-1}^z)^{-1}\Sigma_{k|k-1}^{z\tilde{x}} \tag{16}$$

The target $\mu_k^{\tilde{x}}$ and $\Sigma_k^{\tilde{x}}$ can be derived if all the element values in Equation (15) and (16) are known. All Gaussian filters compute/approximate these terms by alternating between predicting (Time update) and correcting (Measurement update) steps:

1)**Time update (Predictor):**
In the time update step, the predictive distribution $p(\tilde{x}_k|z_{1:k-1})$ is computed via:

$$p(\tilde{x}_k|z_{1:k-1}) = \int p(\tilde{x}_k|\tilde{x}_{k-1})p(\tilde{x}_{k-1}|z_{1:k-1})d\tilde{x}_{k-1} \tag{17}$$

Assume a Gaussian filter distribution $p(\tilde{x}_{k-1}|z_{1:k-1}) = \mathcal{N}(\mu_{k-1}^{\tilde{x}}, \Sigma_{k-1}^{\tilde{x}})$ is given, otherwise the initial state distribution of $p(\tilde{x}_0)$ is employed. Note that the transition probability $p(\tilde{x}_k|\tilde{x}_{k-1})$ can be exactly computed through Equations (5) and (11)-(13) by treating $\tilde{x}_{k-1}$ as $\tilde{x}_*$. The time update equations are listed in Table 1.

As can be seen from Table 1, the state prediction is the sum of Equation (5) and (11), i.e. SINDy estimate plus GP estimate, whereas the state covariance is estimated from GP alone. Hence, the state prediction $\mu_{k|k-1}^{\tilde{x}}$ and covariance $\Sigma_{k|k-1}^{\tilde{x}}$ are obtained.

Table 1. Time update equations

State prediction ($\mu_{k|k-1}^{\tilde{x}}$) : $Equation(5) + (11)$	
State covariance ($\Sigma_{k|k-1}^{\tilde{x}}$) : $Equation(12)$	(13)

2)**Measurement update (Corrector):**
In the measurement update step, the joint distribution $p(\tilde{x}_k, z_k|z_{1:k-1})$ is computed:

$$p(\tilde{x}_k, z_k|z_{1:k-1}) = p(z_k|z_{1:k-1})p(\tilde{x}_k|z_{1:k-1}) \tag{18}$$

Since a Gaussian distribution $p(\tilde{x}_k|z_{1:k-1}) = \mathcal{N}(\mu_{k|k-1}^{\tilde{x}}, \Sigma_{k|k-1}^{\tilde{x}})$ is approximated from the time update, it remains to compute the covariance $\Sigma_{k|k-1}^{\tilde{x}z}$ and $p(z_k|z_{1:k-1})$:

$$p(z_k|z_{1:k-1}) = \int p(z_k|\tilde{x}_k)p(\tilde{x}_k|z_{1:k-1})d\tilde{x}_k$$

The $p(z_k|\tilde{x}_k)$ is the marginal measurement distribution, which has been described by a simple linear Equation (3) rather than a GP model, whose mean $\mu_{k|k-1}^z = C\mu_{k|k-1}^{\tilde{x}}$ and covariance $\Sigma_{k|k-1}^z = C\Sigma_{k|k-1}^{\tilde{x}}C^T + R$. Similarly, the $\Sigma_{k|k-1}^{\tilde{x}z} = \Sigma_{k|k-1}^{\tilde{x}}C^T$, hence all the values used in Equation (15)-(16) are computed. Noticeably, the measurement update procedure in this case is exactly the one in the Kalman filter, which has been summarized in Table 2. Using these results, the SINDy-GP filter algorithm is derived, so that the WEF has been estimated by an alternating predictor-corrector procedure in each time step.

Table 2. Measurement update equations

Filter gain:	$K_k = \Sigma_{k|k-1}^{\tilde{x}}C^T[C\Sigma_{k|k-1}^{\tilde{x}}C^T + R]^{-1}$
Measurement residual:	$e_k = z_k \quad C\mu_{k|k-1}^{\tilde{x}}$
State update:	$\mu_k^{\tilde{x}} = \mu_{k|k-1}^{\tilde{x}} + K_k e_k$
State covariance update:	$\Sigma_k^{\tilde{x}} = (I \quad K_k C)\Sigma_{k|k-1}^{\tilde{x}}$

6. RESULTS

In this Section, the case study for validating the proposed WEF estimator will be described. To date, common prac-

tice in the literature for the validation of an WEF estimator is to employ a known (linear or non-linear) parametric model of the system hydrodynamics, and the identical model is also used in motion simulations. However, it can be assumed that accurate models are usually not available in practice. Even if an accurate model is available the result may be that the performance of robust algorithms are underestimated compared with those methods that can not handle dynamic uncertainties. In order to avoid the use of same model in both WEC hydrodynamic simulation and the WEF estimation stages, a two-body floating-point absorber (RM3) WEC-Sim model is selected. The linear-based time-domian RM3 WEC-Sim model is one of the U.S. Department of Energy WEC reference models, which is validated via experimental results, can fast accurately approximated linear and weakly non-linear WEC hydrodynamics(Van Rij et al., 2019).

We collect the state x, F_{ex} and F_{pto} observations from $RM3$ WEC-Sim simulations, then the acquired data are used to identify the proposed data-driven model for WEF estimation. The constant damping control and JONSWAP spectrum are employed on PTO system and generation of irregular waves, respectively. For the sake of validating the robustness of proposed method, process noise w and measurement noise ϵ are added to observations, and the value of F_{ex} and F_{pto} are rescaled to the same magnitude of state x. Firstly, a *prior* model is derived with the SINDy algorithm, the candidate functions in the library are product combinations of floater position, acceleration and velocity, together with WEF and PTO force. The validation results and model coefficients are shown in Fig.2 and Fig.3, respectively. It is clear that, the active terms in

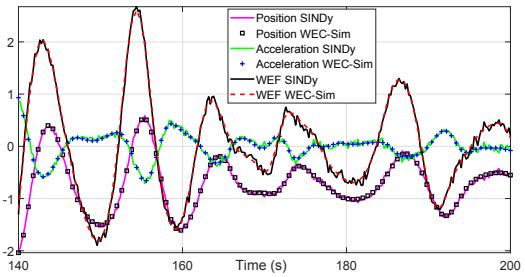

Fig. 2. Comparison between position, acceleration and velocity obtained from WEC-Sim and from the simulation with the SINDy model

the library are sparsely identified,i.e., SINDy attempts to employ as few terms as possible to approximate the target dynamical system. The output of the SINDy model is less smooth compared with the ground truth, due to the fact that all the observations used to train the SINDy model are noisy, along with the input sequences. However the performance of SINDy is accurate, which means that the residual between WEC-Sim and SINDy simulation results is mainly noise rather than un-modeled dynamics. In Fig.4, although the mean of the GP model failed to represent the un-modeled dynamics (with roughly approximation), the GP gives state-dependent uncertainty calculation that can almost cover all the unknown dynamics. This valuable information of uncertainty bound could in turn improve the estimator robustness and accuracy. By combining the

, ,	' Δ p'	' Δ a'	' Δ v'	' Δ WEF'
'1'	[0]	[-0.1037]	[-0.0055]	[-0.1192]
'p'	[0]	[-0.1421]	[-0.0076]	[-0.1605]
'a'	[0.0201]	[-0.1055]	[0.1950]	[0.2894]
'v'	[0.2015]	[0.2437]	[0.0243]	[0.9761]
'pp'	[0]	[0.0033]	[0]	[0.0082]
'pa'	[0]	[0]	[0]	[0]
'pv'	[0]	[-0.0161]	[0]	[-0.0252]
'aa'	[0]	[-0.0059]	[0]	[-0.0116]
'av'	[0]	[-0.0101]	[0]	[-0.0198]
'vv'	[0]	[-0.0054]	[0]	[-0.0138]
'WEF'	[0.0023]	[0.4504]	[0.0398]	[0.8274]
'PTO'	[0]	[0.0507]	[0.0024]	[0.0723]

Fig. 3. The coefficients of SINDy model via sparse regression

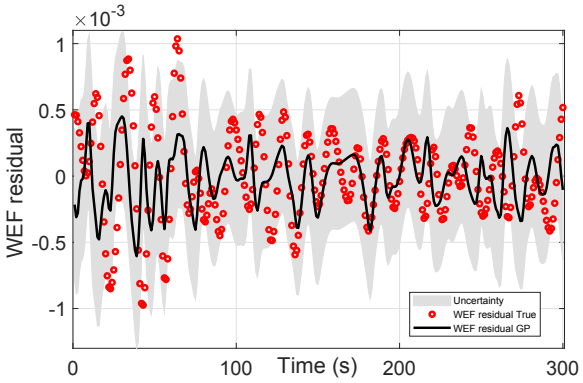

Fig. 4. The obtained residual WEF by the GP model

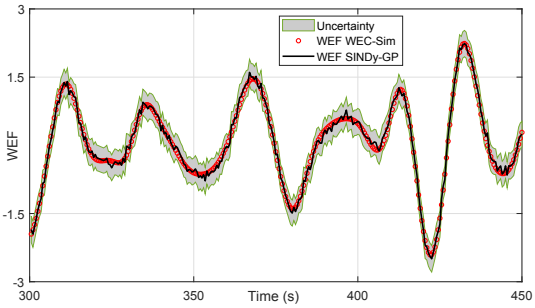

Fig. 5. The obtained WEF by adding SINDy and the GP model

result from SINDy and GP model, the probabilistic model for WEF estimation is derived, where both the mean and uncertainty of the WEC system can be computed. This is clear in Fig.5. By using the alternation of predictor and corrector equations summarized in Table 1 and 2, the F_{ex} can be estimated robustly in real time. As shown in Fig.6, both process and measurement uncertainty can be properly handled, although the mean of the estimates do not always lie centrally, as expected, the variance provided by the proposed estimator can almost grantee the true F_{ex} are lie in its uncertainty bound. Due to limited space of this paper, more comparison with other WEF estimators in term of quantitative analysis, robustness, computational

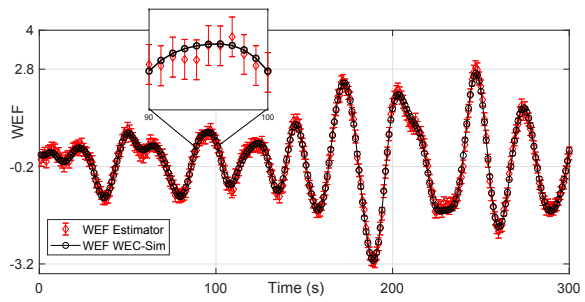

Fig. 6. F_{ex} estimation using the proposed strategy in close-loop evolution, considering both process and measurement noise

complexity and practical tuning procedure,etc., will be considered in the future work.

7. CONCLUSION

Unlike other WEF estimators, which often assume the parametric models of the transition and measurement function are available. This paper proposes a purely data-driven algorithm for WEF estimation, where a probabilistic model is identified from data. This modern modeling method provides more detailed descriptions about the target WEC dynamics compared to a simple parametric linear model that may no longer be validated due to violations of the small wave assumption in practice. The probabilistic model is a combination of SINDy and GP models, which are used to act as the first principles model and unknown dynamical model, respectively. Based on the uncertainty qualification ability provided by the probabilistic model, the calculation of state-dependent distribution can be realized via an analytic moment matching method, which can approximate the uncertainty propagation reliably. The simulation results indicate both accuracy and robustness of the proposed WEF estimator. These advantages render the proposed robust data-driven WEF estimator feasible for real sea implementation.

REFERENCES

Abdelrahman, M. and Patton, R. (2019). Observer-based unknown input estimator of wave excitation force for a wave energy converter. *IEEE Transactions on Control Systems Technology*.

Association, E.O.E. et al. (2010). Oceans of energy european ocean energy roadmap 2010-2050. *Belgium, Brussels*.

Brunton, S.L., Proctor, J.L., and Kutz, J.N. (2016). Discovering governing equations from data by sparse identification of nonlinear dynamical systems. *Proceedings of the National Academy of Sciences*, 113(15), 3932–3937.

Budal, K. and Falnes, J. (1977). Optimum operation of improved wave-power converter. *Mar. Sci. Commun.;(United States)*, 3(2).

Coe, R. and Bacelli, G. (2017). State estimation for advanced control of wave energy converters. Technical report, Marine and Hydrokinetic Data Repository (MHKDR); Sandia National Laboratories.

Cummins, W. (1962). The impulse response function and ship motions. Technical report, David Taylor Model Basin Washington DC.

Deisenroth, M.P., Huber, M.F., and Hanebeck, U.D. (2009). Analytic moment-based Gaussian process filtering. In *Proceedings of the 26th annual international conference on machine learning*, 225–232. ACM.

Deisenroth, M.P. and Ohlsson, H. (2011). A general perspective on Gaussian filtering and smoothing: Explaining current and deriving new algorithms. In *Proceedings of the 2011 American Control Conference*, 1807–1812. IEEE.

Faedo, N., Olaya, S., and Ringwood, J.V. (2017). Optimal control, mpc and mpc-like algorithms for wave energy systems: An overview. *IFAC Journal of Systems and Control*, 1, 37–56.

Fusco, F. and Ringwood, J.V. (2013). A simple and effective real-time controller for wave energy converters. *IEEE Transactions on Sustainable Energy*, 4(1), 21–30.

Ling, B.A. (2019). Development of a model predictive controller for the wave energy converter control competition configuration: Omae2019-95544. In *38th International Conference on Ocean, Offshore and Arctic Engineering ASME OMAE*.

Peña-Sanchez, Y., Windt, C., Davidson, J., and Ringwood, J.V. (2019). A critical comparison of excitation force estimators for wave-energy devices. *IEEE Transactions on Control Systems Technology*, 1–13. doi:10.1109/TCST.2019.2939092.

Rasmussen, C.E. and Williams, C.K. (2006). Gaussian processes for machine learning. 2006. *The MIT Press, Cambridge, MA, USA*, 38, 715–719.

Ringwood, J.V., Bacelli, G., and Fusco, F. (2014). Energy-maximizing control of wave-energy converters: The development of control system technology to optimize their operation. *IEEE Control Systems*, 34(5), 30–55.

Salter, S.H., Taylor, J., and Caldwell, N. (2002). Power conversion mechanisms for wave energy. *Proceedings of the Institution of Mechanical Engineers, Part M: Journal of Engineering for the Maritime Environment*, 216(1), 1–27.

Shi, S., Abdelrahman, M., and Patton, R.J. (2019). Wave excitation force estimation and forecasting for wec power conversion maximisation. In *2019 IEEE/ASME International Conference on Advanced Intelligent Mechatronics (AIM)*, 526–531.

Shi, S., Patton, R.J., Abdelrahman, M., and Liu, Y. (2019). Learning a predictionless resonating controller for wave energy converters configuration: Omae2019-95619. In *38th International Conference on Ocean, Offshore and Arctic Engineering ASME OMAE*.

Shi, S., Patton, R.J., and Liu, Y. (2018). Short-term wave forecasting using Gaussian process for optimal control of wave energy converters. 51(29), 44 – 49. 11th IFAC Conference on Control Applications in Marine Systems, Robotics, and Vehicles CAMS 2018.

Taghipour, R., Perez, T., and Moan, T. (2008). Hybrid frequency–time domain models for dynamic response analysis of marine structures. *Ocean Engineering*, 35(7), 685–705.

Van Rij, J., Yu, Guo, Y., and Coe (2019). A wave energy converter design load case study. *Journal of Marine Science and Engineering*, 7, 250. doi:10.3390/jmse7080250.